www.MaterialsViews.com

Piezoelectric Materials

Piezoelectric-Enhanced Oriented Cobalt Coordinated Peptide Monolayer with Rectification Behavior

*Xinxin Wang, Wen Jiang, Qiang Zheng, Ling Yan, Yiming Jin, Changbao Han, Jie Zhuang, Hong Liu, and Zhou Li**

Electron transfer in biological systems has received great interest and has been widely studied because of the important role it plays in energy/mass conversion and the development of molecular-based electronics.[1] In a photosynthesis system, vectorial electron transfer can be generated by a vertically oriented α-helical peptide bundle whose particular functional groups are located in the membrane.[2] The α-helical peptide has attracted much attention as a universally functional molecule in biological electron-transfer systems, because the macro-dipole moment along the helix axis is large, about 3.5 D per amino-acid residue.[3] Especially in an oriented macro-dipole moment assembly, effective unidirectional electron transfer is expected.

The Langmuir–Blodgett (LB) technique[4] and ring-opening polymerization[5] are the typical techniques for the fabrication of an α-helical peptide monolayer (α-HPM) on a substrate. Self-assembly is also often used for α-HPM fabrication.[6] However, because of the interaction between α-helical peptide dipoles, the antiparallel packing of α-helical peptides is generally preferable to the parallel one.[6d] As a result, the electron flow can be made non-unidirectional.[7] Some researchers have found that the molecular orientation can be adjusted by electrostatic effects. Under an appropriate voltage, Samulski et al. reported on the orientation of a monolayer of α-helical peptides.[8] By applying an external electric field, we were able to create an α-HPM with nonlinear electron flow in our previous study.[9]

Dr. X. Wang, W. Jiang, Dr. Q. Zheng, Y. Jin,
Dr. C. Han, Prof. H. Liu, Prof. Z. Li
Beijing Institute of Nanoenergy and Nanosystems
Chinese Academy of Science
Tower C, Techart Plaza, No. 30 Xueyuan Road
Haidian District, Beijing 10083, P.R. China
E-mail: zli@binn.cas.cn

L. Yan
Key Laboratory for Biomechanics and
Mechanobiology of Ministry of Education
School of Biological Science and Medical Engineering
Beihang University
No. 30 Xueyuan Road
Haidian District, Beijing 10083, P.R. China

Dr. J. Zhuang
Leibniz Institute for Plasma Science and Technology
Felix-Hausdorff-Str. 2, Greifswald 17489, Germany

DOI: 10.1002/smll.201500857

Recently, an innovative approach using a nanogenerator (NG) has been demonstrated for environmentally friendly energy harvesting by converting mechanical energy into electricity. A NG fabricated using a piezoelectric material, namely, ZnO nanowire arrays, has been developed by Wang and co-workers.[10] Using piezoelectric $BaTiO_3$ nanoparticles, Lee et al. have also reported a low-cost, simple, and effective approach to fabricate NGs.[11] These NGs have been demonstrated to successfully power electric devices and equipment. Additionally, a triboelectric NG (TENG) has been studied thoroughly and found to be relying on the coupling of electrostatic induction and triboelectrification. Various applications of TENGs have been developed in recent years.[12,13]

Here, we report an α-HPM fabricated by a piezoelectric field generated from a NG. The α-HPM shows vectorial electron transfer and rectification behavior, whereby an alternating current (AC) signal is changed into a direct current (DC) signal by the α-HPM acting as the electric rectifier. Using this green fabrication method, an oriented α-HPM was prepared owing to the piezoelectric electric field generated by the mechanical motion. This green method could save more energy and was easy to achieve. In addition, the HPM-NG conjugated system has significant potential to be applied in energy conversion, molecular memory devices, nonlinear molecular electronics, and biosensors.

Through a typical solid-phase method, a peptide, Lipo-$LysLeu_2HisLeu_6HisLeu_6$ (peptideKL, **Figure 1**a) was synthesized.[14] The metal ligands were introduced in the peptide sequence using histidines (His) with an imidazole group. Two imidazole groups were arranged on the side surface in the same direction, whereby an α-helix was formed (Figure 1b). This helix was stabilized by the complex of His and metal ions (Figure 1c). At the *C*-terminal of peptideKL, lysine (Lys) was modified with lipoic acid. Circular dichroism (CD) measurements were carried out to analyze the structure of peptideKL in a solution of 2,2,2-trifluoroethanol (TFE) (Figure 1d). A curve-fitting method was used to calculate the fraction α-helix, 59%.[15]

A NG based on $BaTiO_3$ NPs was prepared as the substrate for peptide growth (**Figure 2**a). Through the periodical bending and releasing, driven by a linear motor, the electrical output of the NG was measured (Figure 2). The voltage was about 300 mV at the bending stage.

Furthermore, the piezoelectric poling cell for the fabrication of the peptide monolayer was accomplished by attaching a polydimethylsiloxane (PDMS) frame (30 mm × 15 mm × 8 mm)

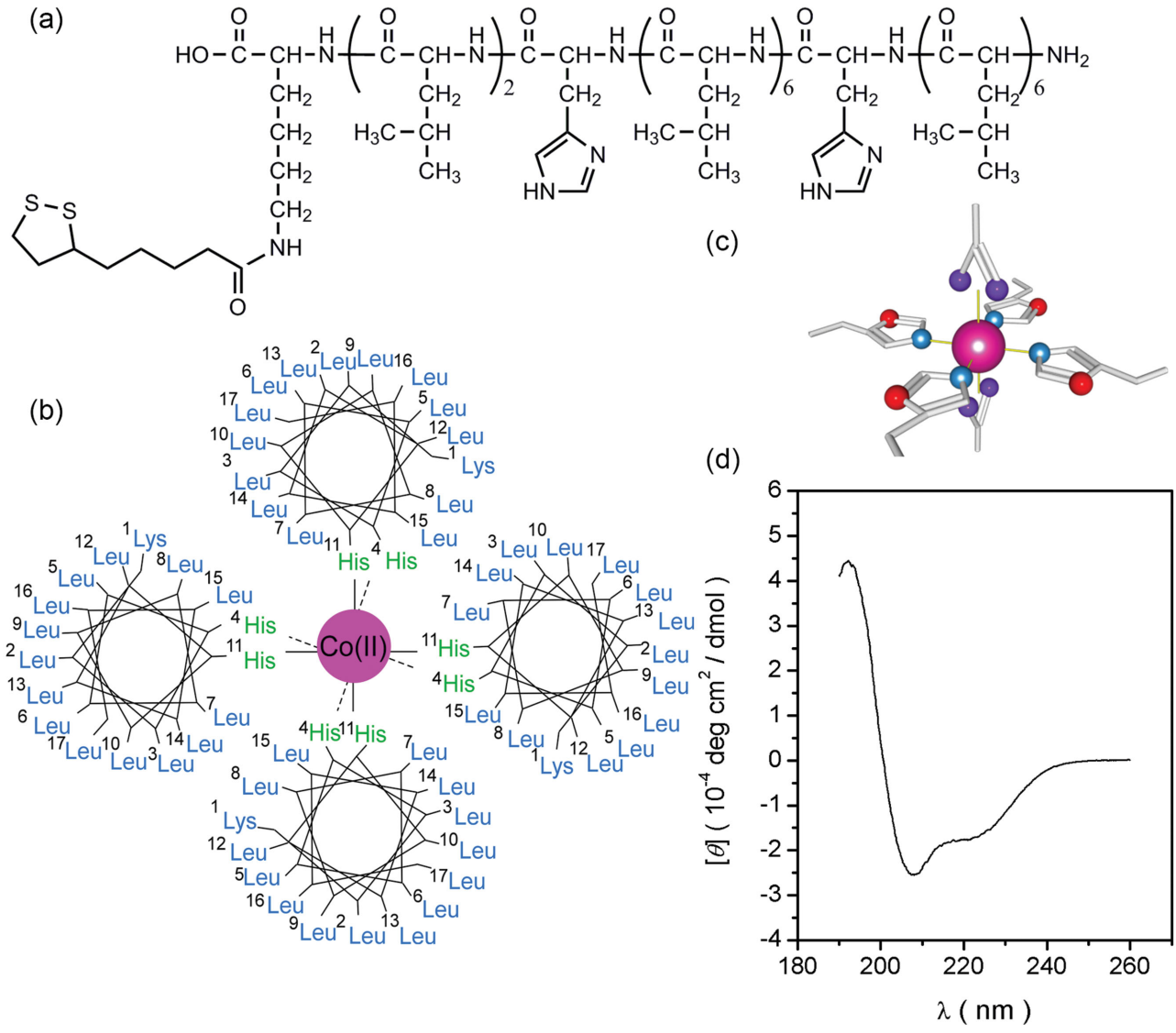

Figure 1. a) Chemical structure of peptideKL. b) Top view and c) bird view of the peptide-Co(II) complex. d) CD spectrum of the peptideKL in TFE.

on one gold electrode of the $BaTiO_3$ NG (Figure 2b). A 0.1 mM TFE solution of peptideKL was placed in the piezoelectric poling cell, the NG was then bent and these conditions were maintained for 12 h to fabricate the peptide monolayers on the electrode. When the NG was bent, the electrode with the positive piezoelectric potential was defined as the positive electrode. The other side was the negative electrode. The KL17_pos and KL17_neg were the monolayers on the positive and negative electrode of the NG, respectively. Afterwards, the NG electrodes were rinsed with TFE three times for 5 minutes. The Co α-HPM layers were prepared using the same procedure. A mixed solution of 0.1 mM peptideKL and Co(II) acetate was prepared in TFE to form Co(II) coordinated monolayers on both the positive and negative electrodes (KL17Co_pos; Figure 2c and KL17Co_neg). The molar ratio of Co to His was 1:4. We also prepared a peptide monolayer on the electrode without bending the NG as a control sample (KL17).

Cyclic voltammetry (CV) was performed to assess the amount of defects in the monolayer as a blocking experiment. The CV measurements were carried out using a supporting electrolyte of 1 M KCl aqueous solution with 1 mM $K_4[Fe(CN)_6]$ (**Figure 3**a). For electrodes with a peptide monolayer without defects CV curves without redox peaks were observed for both the KL17_pos and KL17_neg electrodes. In contrast, clear redox peaks were observed in the absence of a monolayer or when the monolayer contained defects. Our results indicate that the redox probes could not be oxidized/reduced on the KL17_pos and KL17_neg gold electrodes and the peptide on the surface of the electrode was uniformly fixed.

The orientation and the conformation of the peptides on the gold electrode on top of the NG were studied by Fourier Transform Infrared Reflection-Absorption Spectroscopy (FTIR-RAS). The monolayer gave rise to peaks at 1654 and 1545 cm^{-1}, which are typical for amide I and amide II (Figure 3b,c).[16] **Table 1** shows the analyzed results of different monolayers. The calculation method has been reported in a previous paper.[17]

We also measured the helicity of the peptide in the monolayer and in solution. The helicity of the peptide in

www.MaterialsViews.com

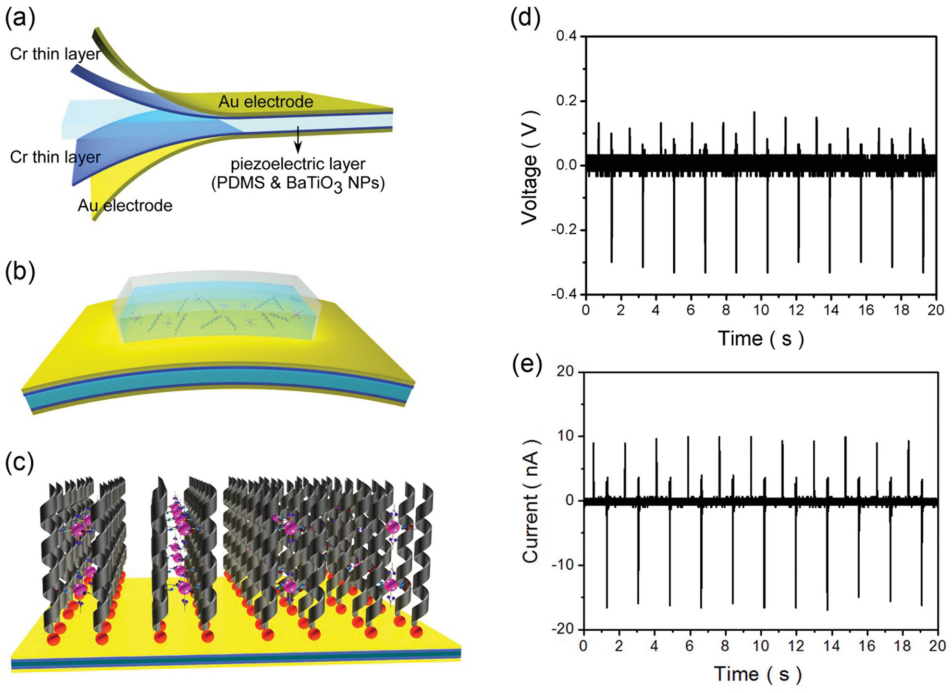

Figure 2. The schematic drawings of: a) the structure of a NG based on $BaTiO_3$ NPs and b) the NG and the piezoelectric poling cell. c) Structure of KL17Co_pos fabricated on the positive electrode. d,e) Electric output signals of the piezoelectric NG during the periodic bending and releasing motions.

the KL17, KL17_pos, and KL17Co_pos monolayers was higher than that in solution. This indicates that the stability of the α-helix was increased by adsorption of the peptide on the positive electrode. On the negative electrode, the helicities of the peptide were 59% and 60% for KL17_neg and KL17Co_neg, respectively. These values were close to that of the peptide in TFE. In the KL17Co_pos, owing to the Co(II)-His complex formation, the helicity was increased to 77%. The tilt angle of the α-helix was decreased from 47° (KL17) to 33° (KL17_pos) by applying a positive piezoelectric potential. Particularly, the tilt angle in KL17Co_pos was 25°, which is smaller than that in the metal-free KL17_pos (33°), which is related to the formation of a Co-His complex. In our research, the peptideKL could self-assemble on the gold surface with lipoic acid at its *C*-terminal. For the KL17Co_pos electrode the electrostatic interaction between the *C*-terminal and positive electrode induced a unidirectional and vertical arrangement of the α-helix, with the assistance of the macro-dipole moment. This process does not occur in the absence of an applied voltage. For the KL17Co_neg electrode the applied potential was negative, which attracts the *N*-terminal by electrostatic interactions, and the *C*-terminal is still attracted by the lipoic acid. In this situation, the helicity decreased and the orientation was destroyed by the interactions between the peptide terminals and the gold electrode. In the FTIR-RAS of KL17Co_pos (Figure 3c), the peak at 1590 cm^{-1} could be assigned to the carbonyl-stretching band of the $CH3COO^-$ group. This implies that the cobalt complex that formed in the peptide bundle was arranged perpendicularly to the electrode surface.

Current (*I*)-voltage (*V*) curves were measured to evaluate the electron transfer process through the peptide monolayer (**Figure 4**). The current response was investigated in a conventional aqueous electrolyte solution (0.1 M KCl, 50 mM triethanolamine (TEOA), and 50 mM methyl viologen (MV^{2+})) as has been reported before.[7b] TEOA and MV^{2+} were the electron donor and acceptor, respectively.

The current response of the KL17 monolayer fabricated on the NG electrode without bending was distinctly different from that of the monolayers prepared on the bent NG electrode. For the non-bent KL17 electrode the current increased independently of the sign of the applied potential (i.e., either a positive or negative bias both induced a current (Figure 4, red line)). Although, when applying a positive sample bias, the current response was slightly smaller than when applying a negative sample bias. For the KL17_pos and KL17Co_pos electrodes, however, the *I*–*V* curves showed a typical asymmetric response (Figure 4, green and navy line). We did not observe a clear current response for the KL17_pos and KL17Co_pos electrodes when applying a positive sample bias; however, the current increased significantly when a negative sample bias was applied. Moreover, KL17Co_pos showed a larger current than the metal-free KL17_pos electrode when applying a similar negative sample bias. KL17_neg showed only a very slight current response when applying either a negative or positive bias compared to those of the KL17, KL17_pos, and KL17Co_pos electrodes.

The drawings in **Scheme 1** show the process of electron transfer through the α-HPM layer. It can be seen that generally antiparallel structures were formed rather than parallel

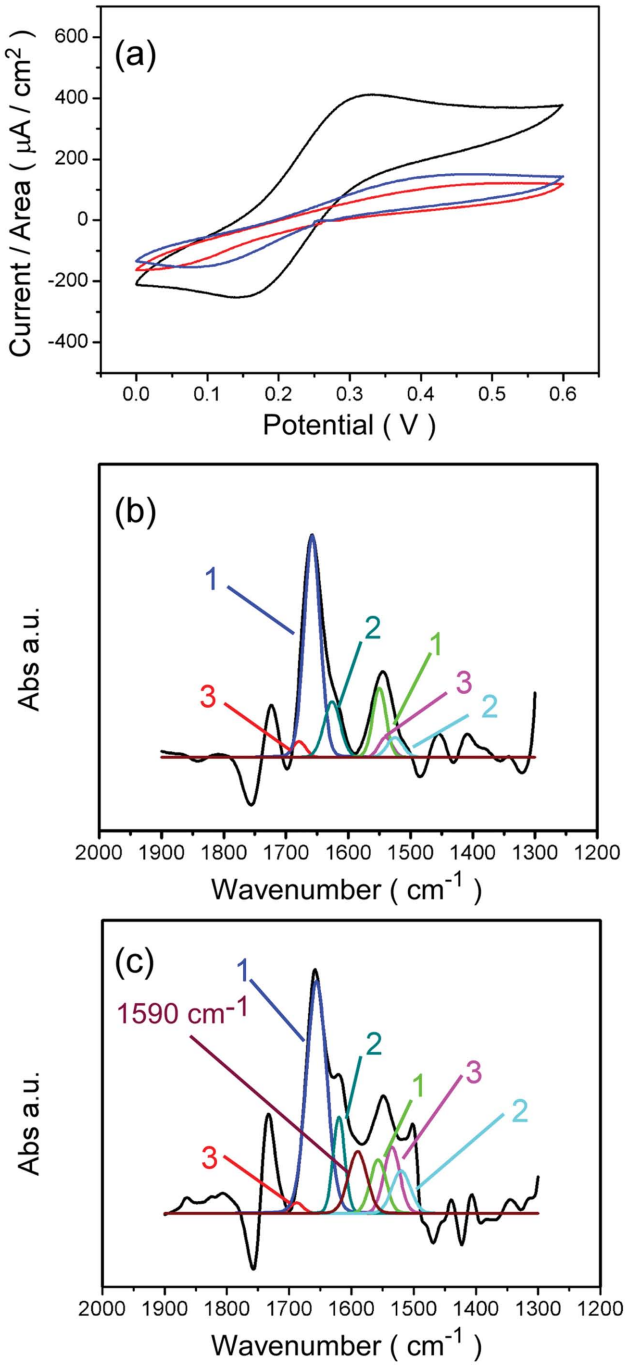

Figure 3. a) CVs of bare NG electrode (black), KL17_pos (red), and KL17_neg (blue). b,c) FTIR-RAS of b) KL17_pos and c) KL17Co_pos.

ones in KL17, because of the interaction between the dipoles of the α-helical peptides. Some reversed α-helical peptides in antiparallel structures of KL17 could also transfer electrons from the monolayer surface to the electrode, which decreased the overall current in the measurement system. In the KL17_pos and KL17Co_pos electrodes the conformation and molecular orientation of the peptide was regular. As a result, a current response could only be observed at negative sample bias. This nonlinear effect in the *I–V* characterization is thus related to the orientational arrangement

Table 1. The calculated results of conformation and tilt angles for the peptide monolayers.

	Conformation [%]			Tilt Angle [°]
	α-helix	β-sheet	random coil	
KL 17	74	10	16	47
KL17_pos	75	20	5	33
KL17_neg	59	37	4	65
KL17Co_pos	79	16	5	25
KL17Co_neg	60	16	24	56

of the macro-dipole moment. Moreover, the KL17Co_pos electrode showed the highest current response, implying that a more efficient electron transfer was achieved with a regular macro-dipole moment, which was influenced by the presence of the Co(II)-His complexes. For the KL17_neg electrode the peptide monolayer showed the lowest helicity and it was not arranged vertically (Table 1, Scheme 1c), which resulted in the peptide layer blocking the electron transfer and, thus, acting as an insulating layer.

When an input AC voltage with an amplitude of 300 mV was applied to the KL17Co_pos electrode (**Figure 5**a), the output showed an obvious negative current of –1.5 μA cm^{-2} and a zero bias on the positive side (Figure 5b), which meant that the electrons could only transfer from the electrode to the surface of the monolayer as a negative current. This result indicates that the KL17Co_pos filtered the positive current like a rectifier, because the oriented macro-dipole moment in the regularly packed α-helical peptide provided an internal electric field that prevents electrons from transferring from the monolayer surface to the electrode. The coupling effect of the metal complexation and the macro-dipole moment also enhances the vectorial electron transfer in KL17Co_pos.

In conclusion, we fabricated an α-HPM with vertical and unidirectional orientation using a piezoelectric field generated by a NG. The molecular orientation was characterized in detail. We also studied the electrochemical properties of the α-HPM and Co(II) α-HPM. Without an applied piezoelectric

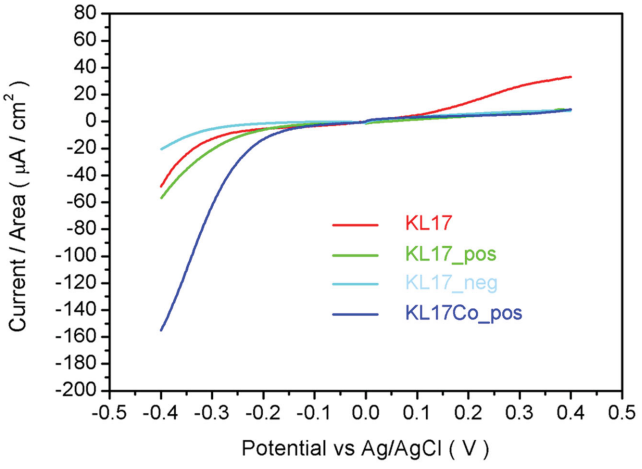

Figure 4. Current (*I*)-voltage (*V*) plots of KL17 (red line), KL17_pos (green line), KL17_neg (cyan line), and KL17Co_pos (navy blue line).

www.MaterialsViews.com

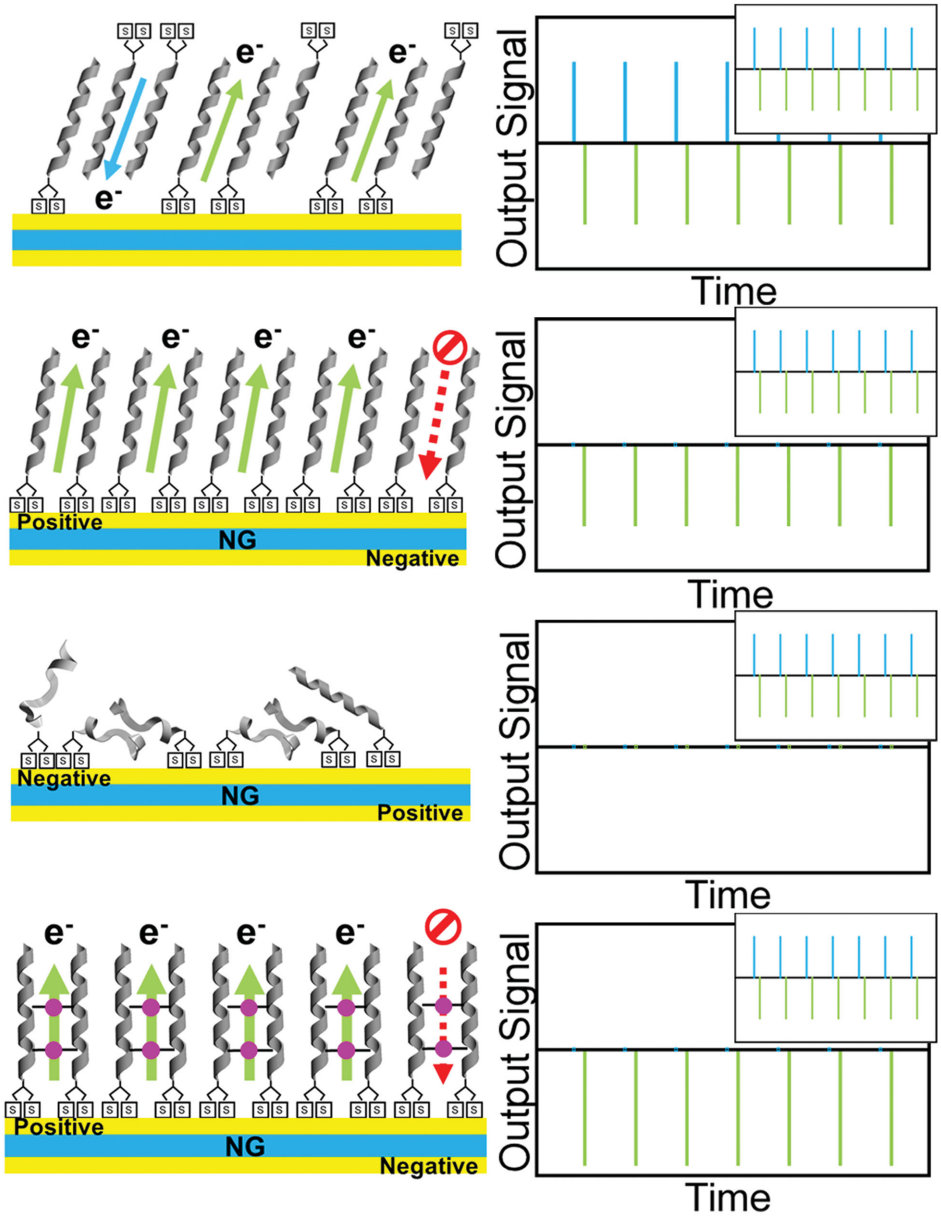

Scheme 1. Schematic diagrams of electron transfer and signal response of the α-helical peptide monolayers: a) KL17, b) KL17_pos, c) KL17_neg, and d) KL17Co_pos when an input signal (inset) was applied. The arrows indicate the direction of the electron flow.

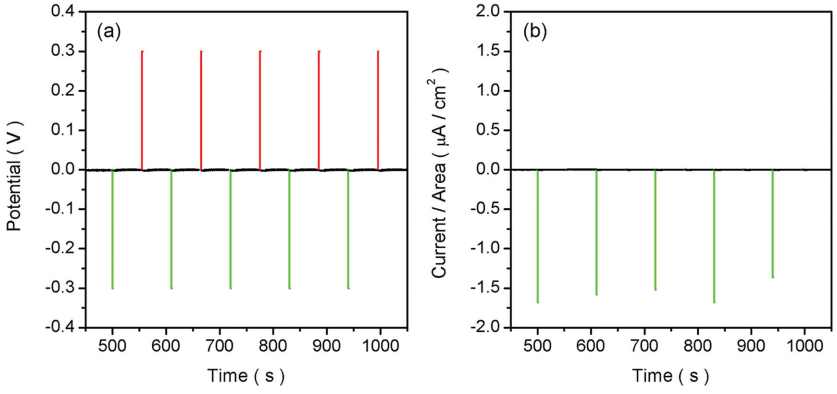

Figure 5. a) Input and b) output characteristics of a KL17Co_pos monolayer.

field α-helical peptides tend to pack in mixed parallel/antiparallel structures. On the positive electrode of the bent nanogenerator, however, the α-helical peptides contain lipoic acid at the *C*-terminals and therefore they formed vertical, stable, and unidirectionally parallel packed bundles. These oriented α-helical bundles, fabricated in the presence of a piezoelectric field, led to electron transfer in the vertical direction through the monolayer and along the macro-dipole moment. The monolayer was therefore able to unidirectionally enhance electron transfer and

rectify an AC signal to a DC signal. We consider this green method of applying a piezoelectric potential from a NG to fabricate asymmetric materials, such as an oriented functional thin layer, to be very effective and economic. Furthermore, this monolayer-NG system can be used in the field of mass/energy conversions as a rectifier. It also has great potential in molecular memories, nonlinear molecular electronic devices, and biosensors.

Experimental Section

Preparation of a Piezoelectric Nanogenerator: A mixture of $BaTiO_3$ NPs (10 wt%) and polydimethylsiloxane (PDMS) elastomer was prepared and molded into a rectangular sheet (50 mm × 25 mm × 1 mm). We heated the NPs and PDMS mixture at 80 °C for 1 h. A thin layer of PDMS was prepared onto a $BaTiO_3$/PDMS sheet by spin-coating (spinning rate: 2000 rpm; time: 40 s) and heated at 80 °C for 15 min to prepare a piezoelectric NG layer. A Cr thin layer (30 nm) and Au electrode layer (50 nm) were respectively deposited onto the upper and lower bottom surfaces of the piezoelectric layer by radio-frequency magnetron sputtering. Under an electric field of 2 kV, the $BaTiO_3$ NG was poled at 100 °C for 10 h.

Spectroscopic Measurements: We measured circular dichroism (CD) using a JASCO J-1500 spectropolarimeter at room temperature. During the experiments, nitrogen gas was flushed through. A 0.1 cm quartz cuvette was used, and the spectral range was set from 190 nm to 260 nm. We prepared a 0.1 mg mL^{-1} peptide 2,2,2-trifluoroethanol (TFE) solution. 16 consecutive scans were carried out and averaged to obtain the CD spectrum in Figure 1d.

Fourier Transform Infrared Reflection-Absorption Spectra (FTIR-RAS) measurements were carried out to investigate the orientational and conformational characteristics of the α-HPMs using a Bruker Tensor II. The incident angle was 80°.

Electrochemical Measurements: We investigated the electrochemical properties of the α-HPMs using an electrochemical workstation at room temperature, with a conventional three-electrode setup. Here, the working electrode was the α-HPM fixed on gold electrode, the reference electrode was a Ag/AgCl standard electrode, and the counter electrode was a platinum wire. All potentials were measured with respect to the reference electrode. For the electrochemical measurements the area of the working electrode was set at 0.785 cm^2. All aqueous solutions in the experiment were treated by vacuum de-aeration firstly.

Supporting Information

Supporting Information is available from the Wiley Online Library or from the author.

Acknowledgements

This work was supported by the NSFC 31200702, Beijing Municipal NSF 7132121, the "Thousand Talents" program for pioneer researchers and his innovation team, Beijing Nova Program Z121103002512019, and Beijing Municipal Science & Technology Commission Z131100006013004. Dr. Xinxin Wang and Wen Jiang contributed equally to this work.

Figure 2 was updated on October 7, 2015.

[1] A. Paul, S. Bezer, R. Venkatramani, L. Kocsis, E. Wierzbinski, A. Balaeff, S. Keinan, D. N. Beratan, C. Achim, D. H. Waldeck, *J. Am. Chem. Soc.* **2009**, *131*, 6498.
[2] a) J. Deisenhofer, O. Epp, K. Miki, R. Huber, H. Michel, *Nature* **1985**, *318*, 618; b) G. Babcock, *Proc. Natl. Acad. Sci. USA* **1993**, *90*, 10893.
[3] A. Wada, *Adv. Biophys.* **1976**, *9*, 1.
[4] a) K. Kishihara, T. Kinoshita, T. Mori, Y. Okahata, *Chem. Lett.* **1998**, 951; b) T. Doi, T. Kinoshita, Y. Tsujita, H. Yoshimizu, *Bull. Chem. Soc. Jpn.* **2001**, *74*, 421; c) N. Higashi, T. Koga, M. Niwa, *Langmuir* **2000**, *16*, 3482.
[5] a) R. H. Wieringa, A. J. Schouten, *Macromolecules* **1996**, *29*, 3032; b) A. Heise, H. Menzel, H. Yim, M. D. Foster, R. H. Wieringa, A. J. Schouten, V. Reb, M. Stamm, *Langmuir* **1997**, *13*, 723.
[6] a) K. Fujita, N. Bunjes, K. Nakajima, M. Hara, H. Sasabe, W. Knoll, *Langmuir* **1998**, *14*, 6167; b) M. Niwa, T. Murata, M. Kitamatsu, T. Matsumoto, N. Higashi, *J. Mater. Chem.* **1999**, *9*, 343; c) K. Yanagisawa, T. Morita, S. Kimura, *J. Am. Chem. Soc.* **2004**, *126*, 12780; d) N. Higashi, J. Kawahara, M. Niwa, *J. Colloid Interface Sci.* **2005**, *288*, 83.
[7] a) X. Wang, K. Nagata, M. Higuchi, *Langmuir* **2011**, *27*, 12569; b) X. Wang, K. Nagata, M. Higuchi, *Thin Solid Films* **2012**, *520*, 2884.
[8] C. G. Worley, R. W. Linton, E. T. Samulski, *Langmuir* **1995**, *11*, 3805.
[9] X. Wang, S. Fukuoka, R. Tsukigawara, K. Nagata, M. Higuchi, *J. Colloid Interface Sci.* **2012**, *390*, 54.
[10] a) Z. L. Wang, J. H. Song, *Science* **2006**, *312*, 242; b) Z. Li, G. Zhu, R. Yang, A. C. Wang, Z. L. Wang, *Adv. Mater.* **2010**, *22*, 2534.
[11] K. Park, M. Lee, Y. Liu, S. Moon, G. T. Hwang, G. Zhu, J. E. Kim, S. O. Kim, D. K. Kim, Z. L. Wang, K. J. Lee, *Adv. Mater.* **2012**, *24*, 2999.
[12] a) F. R. Fan, Z. Q. Tian, Z. L. Wang, *Nano Energy* **2012**, *1*, 328; b) X. S. Zhang, M. D. Han, R. X. Wang, B. Meng, F. Y. Zhu, X. M. Sun, W. Hu, W. Wang, Z. H. Li, H. X. Zhang, *Nano Energy* **2014**, *4*, 123.
[13] a) T. C. Hou, Y. Yang, H. Zhang, J. Chen, L. J. Chen, Z. L. Wang, *Nano Energy* **2013**, *2*, 856; b) Q. Zheng, B. J. Shi, F. R. Fan, X. X. Wang, L. Yan, W. W. Yuan, S. H. Wang, H. Liu, Z. Li, Z. L. Wang, *Adv. Mater.* **2014**, *26*, 5851.
[14] W. C. Can, P. D. White, *Fmoc Solid Synthesis: A Protocol Approach*, Oxford University Press, UK **2000**.
[15] N. Greenfield, G. D. Fasman, *Biochemistry* **1969**, *8*, 4108.
[16] E. P. Enriquez, E. T. Samulski, *Mater. Res. Soc. Symp. Proc.* **1992**, *255*, 423.
[17] X. Wang, K. Nagata, M. Higuchi, *Thin Solid Films* **2012**, *520*, 2884.

Received: March 30, 2015
Revised: June 4, 2015
Published online: July 14, 2015

